

Reproducible cavitation activity in water-particle suspensions

Bram M. Borkent, Manish Arora, and Claus-Dieter Ohl^{a)}

Faculty of Science and Technology, Physics of Fluids, University of Twente,
P.O. Box 217, 7500 AE Enschede, The Netherlands

(Received 1 October 2006; revised 23 December 2006; accepted 2 January 2007)

The study of cavitation inception in liquids rarely yields reproducible data, unless special control is taken on the cleanliness of the experimental environment. In this paper, an experimental technique is demonstrated which allows repeatable measurements of cavitation activity in liquid-particle suspensions. In addition, the method is noninvasive: cavitation bubbles are generated using a shock-wave generator, and they are photographed using a digital camera. The cavitation activity is obtained after suitable image processing steps. From these measurements, the importance of the particle's surface structure and its chemical composition is revealed, with polystyrene and polyamide particles generating the highest yields. Further findings are that cavitation nuclei become depleted with an increasing number of experiments, and the existence of nuclei with varying negative pressure thresholds. Finally, a decrease of the cavitation yield is achieved by prepressurization of the suspension—indicating that the cavitation nuclei are gaseous. © 2007 Acoustical Society of America. [DOI: 10.1121/1.2436646]

PACS number(s): 43.35.Ei [AJS]

Pages: 1406–1412

I. INTRODUCTION

The discrepancy between the theoretical tensile strength of pure water and the much lower values reported in various cavitation experiments has been attributed to the presence of cavitation nuclei. Harvey *et al.*¹ suggested that stable, minute gas nuclei are present in cavities on the solid surfaces of suspended particles, and that such cavities could act as nucleation sources. Greenspan and Tschiegg² reported that removing particles larger than 0.2 μm in diameter increased the tensile strength of water to about 200 bar. The hypothesis of Harvey *et al.* developed over several years into the so-called “crevice model”^{3–7} which predicts the acoustic cavitation threshold required to nucleate a vapor cavity from a mote, and the threshold's dependency on bulk liquid properties and crevice attributes such as size, wettability, and geometry.

The experiments^{2,3,8} revealed that cavitation inception depends not only on various liquid properties but also on acoustic parameters such as pulse duration, frequency and the geometric form of the sound field, and (if present) the number of cavitation nuclei and their respective nuclei properties. The latter observation stimulated investigations into the role played by controlled amounts of impurities, such as suspended particles.^{9–14} As a result of that work it was recognized that the method used to determine whether a cavitation event has happened can play a crucial role in determining cavitation thresholds. In the majority of experiments an active detector is used^{9–11,13,14} which consists of a focused transducer operated in pulse-echo mode, typically at 30 MHz (see, for example, Madanshetty *et al.*^{13,14} for details). However, this invasive method affects the cavitation process,¹⁴ for example the acoustic field can convect the particles into the cavitation zone through acoustic radiation forces, and high acoustic frequencies might set particles into oscillatory

motion. The latter could stimulate the formation and subsequent merging of surface bubbles into microscale cavities, which has been termed acoustic coaxing.^{10,14} This hypothesis is also put forward in a more recent study in which a Keller-vortex flow system is used to induce cavitation on microparticles.¹²

Cavitation experiments, when performed under uncontrolled lab conditions, are usually difficult to reproduce, see, for example, the comments of Strasberg in 1959.³ His data showed a “surprising” mean deviation of 10%–15% for 10–20 measurements with unchanged experimental conditions. Madanshetty *et al.*¹⁴ and Deng *et al.*¹¹ suggest that cavitation thresholds are strongly influenced by the cleanliness of the system. They both stress the importance of monitoring and accounting for fine details in the liquid preparation and handling. Thus great experimental care has to be taken to set up the nuclei environment in order to obtain repeatable cavitation measurements. Still, cavitation threshold measurements typically have a standard deviation of about 15%, which is regarded as good; see, for example, Atchley *et al.*¹⁵

In the present work we emphasize the reproducibility of the experiment. This addresses the fact that the results have been reproduced in our lab a few months later with freshly prepared particle-water suspensions. Thus, we expect that this technique is a suitable method to compare cavitation activity—within the later specified error margins—also in different groups.

Given that most of the problems faced in cavitation experiments are related to the invasiveness of the cavitation detector and the cleanliness of the nuclei environment, we designed a method which overcomes both. In this study, we make use of a single acoustic cycle from a shock wave generator to nucleate cavitation bubbles in an ultraclean environment. Since the shock wave passage takes only a few microseconds, the interaction of the acoustic signal with the

^{a)}Electronic mail: c.d.ohl@tnw.utwente.nl

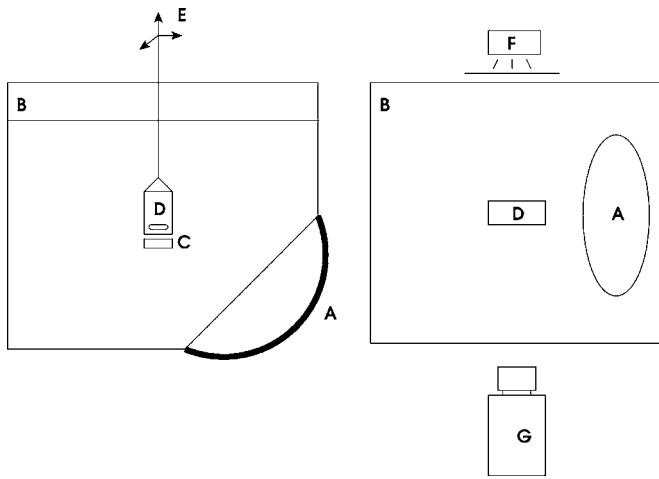


FIG. 1. Side and top view (respectively, left and right) of the experimental setup. A: shock-wave generator, B: water tank, C: magnetic stirrer, D: flask with particle suspension, E: translation stage, F: flash light, and G: camera.

cavitation bubbles is reduced to a minimum which distinguishes this approach from the ones presented in Refs. 2, 3, 8–11, and 13. In addition, we detect cavitation bubbles optically, thus quantitative and noninvasive. With this method we showed previously that cavitation bubbles nucleate on the microparticles itself and, as a direct consequence, the particles are accelerated away with velocities up to tens of meters per second.¹⁶ In contrast, we report here on the depletion of cavitation nuclei due to both the nucleation event itself and prepressurization of the particles. Finally, we report how new sets of cavitation nuclei can be activated by increasing the tensile stress in the liquid in a stepwise manner.

II. MATERIALS AND METHODS

A. Experimental setup

The noninvasive technique to detect cavitation has evolved from a prior experiment discussed in Arora *et al.*¹⁶ Cavitation is induced by a focused shock wave source and is detected with a camera, see Fig. 1. The shock wave source is attached at an angle of 45° in one of the walls of a large container filled with approximately 50 l of partially degassed demineralized water (~ 3 mg/l O_2 concentration at a temperature of approximately $20^\circ C$).

The probe suspension is contained within a polystyrene sterile flask (75 ml, EasyFlask, Nunclon). This is positioned with its center aligned with the acoustic focus of the shock wave source using an xyz -translation stage. A watertight magnetic stirrer (Telemodul 90407, Variomag) located below the flask is mixing the suspension in the flask homogeneously with a glass-coated magnet. Before submerging the flask in the basin its content is sealed with a foil (Parafilm, American National Can, Chicago). Here, care is taken that no air bubbles become entrapped while closing the seal.

Shock waves are generated with a focused piezoelectric source which is a slightly modified extracorporeal lithotripter (Piezolith 3000, Wolf GmbH). The strength of the applied tensile stress is set through the discharge voltage ranging from 0 to 9 kV on the piezoelectric transducers. A typical pressure profile (5 kV discharge voltage) *inside* the polysty-

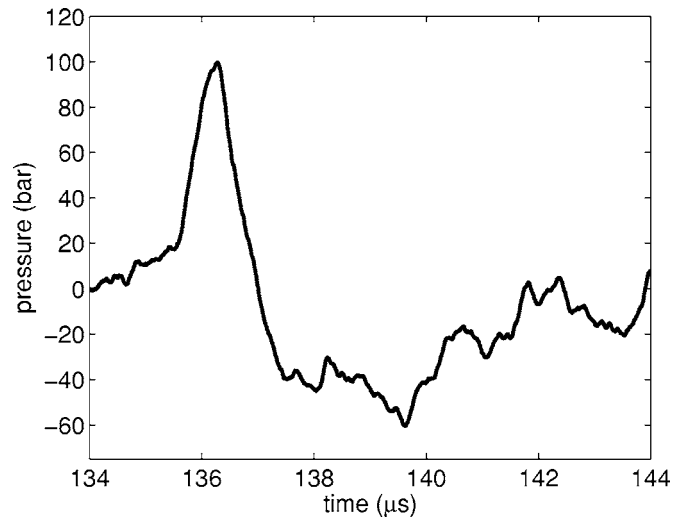


FIG. 2. Pressure as a function of time as recorded inside the flask (without particles) with the fiber optic probe hydrophone FOPH-500 for a charging voltage of 5 kV. The time $t=0$ corresponds to the start of the lithotripter pulse.

rene flask is shown in Fig. 2. The pressure pulse has been recorded with a calibrated glass fiber hydrophone (FOPH-500, RP Acoustics) located inside the sealed flask and close to the acoustic focus point, which is marked by two crossing laser diodes. The measurement shows that the travel time for the pressure wave from the front shell to the acoustic focus is approximately $136 \mu s$. Once the acoustic wave arrives, a steep overpressure-peak (maximum of 100 bar, half-width of $1 \mu s$) is followed by a more elongated tensile wave (minimum of -60 bar, $5 \mu s$ duration). During the latter period the threshold pressure is exceeded and cavitation bubbles are created (Fig. 3). If sufficient cavitation nuclei are present, an approximately cigar-like cavitation cluster is found.¹⁷

Bearing in mind that each expanding and collapsing bubble is acting as an acoustic source, the shape of the pressure wave following the positive peak in Fig. 2 may vary strongly with cavitation activity.¹⁸

The bubble activity is illuminated with a flash lamp (Strobolume 1540, General Radio) positioned behind a diffuser and photographed with a single frame from a digital charged-coupled device camera (Pulnix TM-6710, Alzenau,

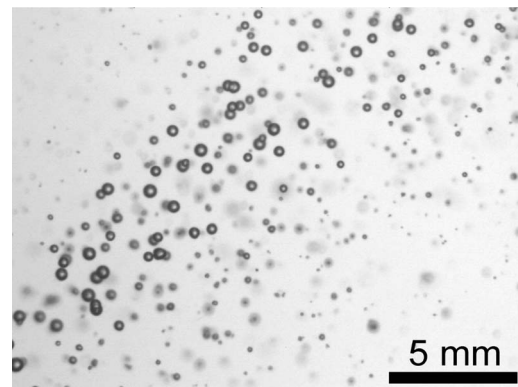


FIG. 3. Typical bubble cloud which appears approximately $14 \mu s$ after passage of the tensile wave (Fig. 2) inside of the flask. Settings: 10^4 particles/75 ml and 5 kV discharge voltage.

Germany). The camera is equipped with a macro lens (Makro-Planar T*2.8/60, Carl Zeiss) and placed around 30 cm from the acoustic focus, which is just outside the water tank. The devices are triggered with a home-made delay generator. The diffuse backillumination provides a good contrast for detecting the bubbles; they are imaged as dark dishes (Fig. 3). The spatial resolution of the images obtained is $32.1 \pm 0.1 \mu\text{m}$ per pixel, resulting in an image area of $15.4 \times 20.6 \text{ mm}^2$. In this image a region of interest (ROI) is selected parallel to the direction of the shock wave propagation being 45° to the horizontal. Bubbles in this ROI are segmented, counted, and analyzed with standard image processing tools (MATLAB, The Mathworks, Natick, MA). To limit the analysis to bubbles within a certain depth range a threshold technique is applied on the bubble border. Bubbles imaged in focus possess a strong gray scale gradient at their edge. Bubbles positioned away from the object plane are imaged with a lower magnitude of the edge gradient. Applying a threshold filter on the averaged gradient of the bubble boundary allows the detection algorithm to limit the counting of bubbles within a fixed depth. This depth has been determined by moving an artificial bubble object back and forth in the imaged volume. It was obtained that the bubble counting algorithm limits the detection depth to 8.0 mm.

B. Liquid handling

Stock solutions of the particles were made in test tubes and their number densities were determined with a Neubauer cell-counting chamber under the microscope. The corresponding volume containing 10^4 particles was pipetted from the test tube with a micropipette into the sterile 75 ml flask. Then, the flasks are filled up to their rim with Milli-Q water and sealed carefully. After placing the flask in the holder at the acoustic focus a shock wave is generated. The bubble activity is recorded approximately $14 \mu\text{s}$ after the passage of the tensile wave through the focus. To check for the water quality of the suspending liquid control experiments were conducted. Only if the flasks containing pure Milli-Q water showed less than five cavitation bubbles in the field of view the water was considered appropriately clean.

In the case of prepressurization (Sec. III C) the suspension was first introduced into a pressure chamber. This consists of a stainless steel cylinder having a maximum volume of 40 ml. The liquid in the cylinder is pressurized with a gas tight piston connected to the labs high pressure air supply. First, the liquid handling system is gently flushed with the suspension. Thereby, it was verified that most bubbles in this system are removed. Then, 40 ml of the suspension are sucked into the cylinder and pressurized with 3 or 5 bar absolute pressure for 15 min. In the control experiment all liquid handling steps were conducted in the same way with the exception of pressurizing the chamber. After 15 min the suspension was pushed smoothly out of the chamber into the flask and an additional volume of 35 ml of partly degassed Milli-Q water with no particles is gently added to fill up the flask, which is then sealed and put into the water tank.

C. Estimation of the cavitation yield

The cavitation yield, α , is defined as the percentage of particles in the acoustic volume which develop into cavitation bubbles, i.e.,

$$\alpha = \frac{N_{\text{bub}}}{N_{\text{particles}}} \times 100 \% . \quad (1)$$

Here, N_{bub} is the number of imaged bubbles and $N_{\text{particles}}$ is the number of particles. The acoustic volume is the volume in the flask where the pressure becomes low enough such that cavitation bubbles become visible. Although the particles are distributed homogeneously in the flask, it is important to stress that the negative pressure amplitude varies strongly in space. Thus, not all of the particles in the acoustic volume can develop into cavitation bubbles. To estimate this acoustically active volume we sum up many images with bubble activity. This averaged image reveals that bubbles appear in an approximately cylindrical region with its central axis aligned with the acoustic pathway: The cylinder length is $14.2 \pm 0.1 \text{ mm}$ and its diameter is $7.3 \pm 0.1 \text{ mm}$ leading to an optically registered acoustic volume as $0.59 \pm 0.02 \text{ cm}^3$. Clearly, these values vary with the applied acoustic pressure but here we limit to the case of 5 kV discharge voltage (corresponding to -60 bar peak tensile stress, see Fig. 2). With the number density of 133 particles/ml given and the assumption of a homogeneous distribution of particles, approximately 78 ± 3 particles are present in the optically registered acoustic volume. For instance, in the first shot of Fig. 6 66 bubbles were counted resulting into a cavitation yield of $\alpha = 85 \pm 3\%$. Thus, most of the particles serve as a cavitation nucleus.

III. RESULTS

The key request of the experiment was that a quantitative measure of cavitation activity of a controlled amount of particles could be obtained *in a reproducible way*. Reproducibility in cavitation experiments is a notorious problem since many factors may stimulate or impose nucleation, especially contamination. In the end, it was found that reliable quantitative data could be obtained by counting the number of bubbles produced by a controlled number of particles in a fixed volume at given shock wave settings while carefully handling the liquids and ultrapure water conditions.

A. Cavitation activity of microparticles

First we investigated different types of particles from which we select one type for further quantitative studies. Figure 4 depicts the number of cavitation events per particle for the ones listed in Table I. Here 10^4 particles per flask, thus 1.3×10^2 per ml, have been prepared and the shock wave generator has been operated from 1 to 5 kV discharge voltage with steps of 1 kV. (The pressure pulse corresponding to 5 kV discharge voltage is depicted in Fig. 2 and has a peak negative pressure of -60 bar .) The total number of bubbles, nucleated in these five subsequent shots, is depicted in Fig. 4. Clearly, polyamide and polystyrene enhance cavi-

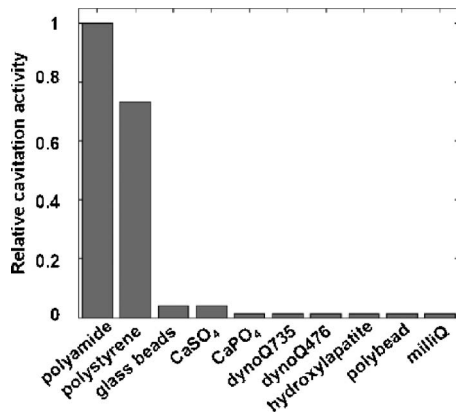


FIG. 4. Relative cavitation activity for different particles suspended in Milli-Q water. The control with the plain suspension liquid gives a count of 0.01.

tation significantly, while the other studied particles (either hydrophilic or covered with surfactants) show only cavitation activity similar to the plain liquid (Milli-Q water). Polyamide and polystyrene particles differ from the other particles as both can be categorized as hydrophobic and rough-structured on the surface. Interestingly, polyamide particles show more cavitation activity than polystyrene. This is surprising since polystyrene (consisting of methyl-groups and phenyl-rings) can be assessed as more hydrophobic than polyamide (which contains many polar amide-groups) and second because the polystyrene particles have around 40 times as much surface area compared with the relatively small polyamide particle, where cavitation nuclei could be entrapped (provided that necessary conditions are satisfied). On the other hand, scanning electron microscopy reveals that polyamide particles have a much rougher surface structure,

at least on the microscale as compared to polystyrene (Fig. 5). Thus, the higher surface roughness of polyamide may facilitate the entrapment and stabilization of gas pockets on the surface. The further studies are conducted with the polyamide particles.

B. Depletion of cavitation activity

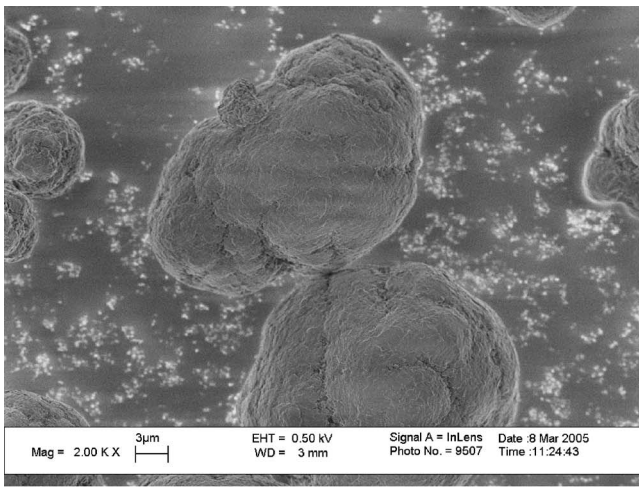
1. Effect of repetitive tensile waves

In the next experiment the effect of multiple pressure waves on the cavitation activity was investigated. 10^4 polyamide particles were suspended in a flask, and 40 subsequent waves at 5 kV discharge voltage (-60 bar peak negative pressure) were applied. The experiment was repeated three times and the number of cavitation bubbles measured. From the average number of bubbles, the mean percentage of nucleated particles per shot was calculated as the cavitation yield, α , and is shown in Fig. 6.

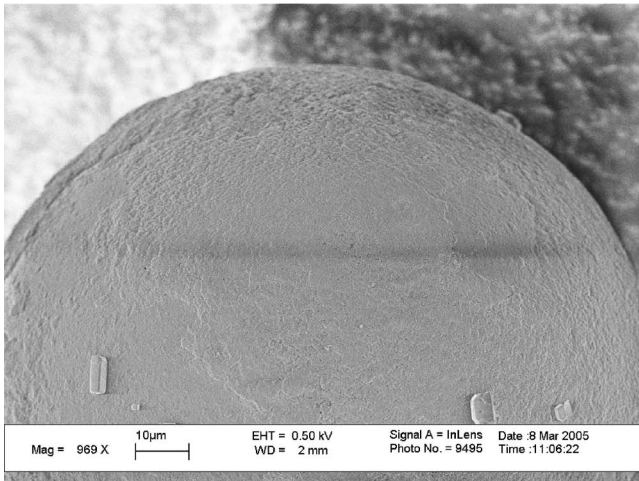
We find a decreasing number of cavitation events with a low variability between experiments, thus high reproducibility. Interestingly, it is found that the number of particles which can be nucleated decreases per shot. This can be explained that each particle has a limited number of nuclei which finally become used up. Additionally, the waiting time between two shots was varied from 10 to 60 s for the circles and the squares in Fig. 6, respectively. Cavitation yield is unaffected by the time interval. The dissolution time for the gaseous remains from cavitation bubbles can be estimated for bubbles reaching a maximum diameter of $400 \mu\text{m}$ during $40 \mu\text{s}$ in water saturated with air at room temperature. A bubble will thereby collect approximately 1.1×10^{12} g of air,¹⁷ which is equivalent to a bubble of $6 \mu\text{m}$ equilibrium radius. These sized bubbles again dissolve within 1.2 s, see,

TABLE I. Characterization of the particles investigated in this study on cavitation activity. An asterisk (*) behind the mean diameter indicates the manufacturers specification. In the other cases the particle sizes were determined with a microscope in the lab.

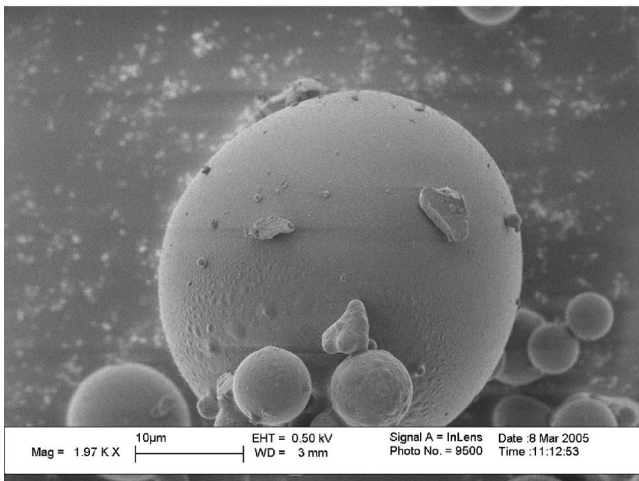
Particle name	Mean diameter (μm)	Features	Manufacturer (product number)
Hollow glass spheres (glass oxide)	11*	Hydrophilic, smooth surface	Potters Industries (110P8)
Polyamide seeding particles	20*	Hydrophobic, rough surface structure	Dantec Dynamics GmbH (80A4011)
Polystyrene-2% divinylbenzene	80–150*	Hydrophobic, rough surface structure	Serva GmbH
Dynosphere Q735, from Ref. 12	40	Hydrophilic, with hydroxyl groups	Dyno Particles AS, Norway (EXP-SS-42.3-RSH)
Dynosphere Q476, from Ref. 12	3.0*	Hydrophilic, smooth surface	Dyno Particles AS, Norway (EXP-SA-3.2-RNI)
Polybead polystyrene microspheres	1.00*	Filled with water, surfactant on surface	Polysciences
Hydroxylapatite ($\text{Ca}_{10}(\text{OH})_2(\text{PO}_4)_6$)	10–100	Biocompatible, slow-dissolving salt	Sigma Aldrich (289396)
β -tri-Calcium phosphate hydroxide ($\text{Ca}_3(\text{PO}_4)_3$)	5–10	Slow-dissolving salt	Fluka (21218)
Calcium sulphate Dihydrate ($\text{CaSO}_4 \cdot \text{H}_2\text{O}$)	10–100	Slow-dissolving salt	Sigma Aldrich (255548)



(a)



(b)



(c)

FIG. 5. SEM pictures of (a) polyamide, (b) polystyrene, and (c) glass spheres: Further specifications are in Table I.

for example, Refs. 19 and 20. Thus, a waiting time between two experiments of 10 s assures that gaseous remains from prior cavitation activity have dissolved.

2. Effect of tensile stress level

If one thinks of cavitation nuclei as becoming “used up” after nucleation, it is interesting to investigate what would

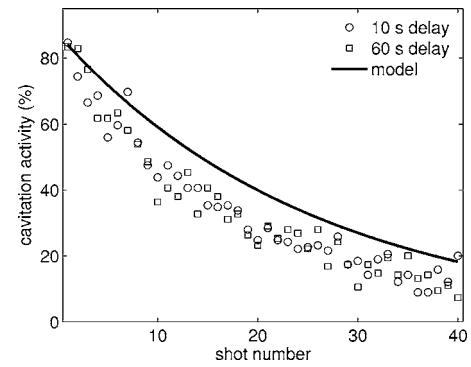


FIG. 6. Cavitation activity given as the percentage of particles that lead to a cavitation event. Each data point is the mean of three experiments. The waiting time of 10 s (circles) and 60 s (squares) has no effect on the cavitation yield. The line shows the values as calculated by the model, Eq. (3), with no adjustable parameter.

happen when the discharge voltage (and thus the tensile stress) is increased stepwise. Are we able to activate a new population of nuclei by applying higher tensile stresses? To answer this question, an experiment similar to the previous one has been performed, but now beginning with a discharge voltage of 4 kV and after 20 shots followed by 20 shots of 5 kV. This was repeated three times and the result is plotted in Fig. 7.

During the first 20 shots the nuclei which can be activated with a 4 kV discharge voltage are growing into cavitation bubbles. The trend of decrease in the cavitation yield resembles the one as depicted in Fig. 6. However, if after 20 shots the acoustic tensile stress is increased, more bubbles become visible, hence, a new set of nuclei is triggered. With the higher tensile stress the number of bubbles again starts to decrease for successive shots.

C. Prepressurization

The crevice model⁷ predicts that a pressurization of the suspension will force the meniscus of the gaseous nuclei to a more convex shape, until it reaches the advancing contact angle. An increased or prolonged pressurization will move the meniscus of the interface toward the apex of the assumed conical crevice: The bubble shrinks and liquid moves into the crevice. Here, the question is addressed if preexisting nuclei on the particles can be affected by pressurization of

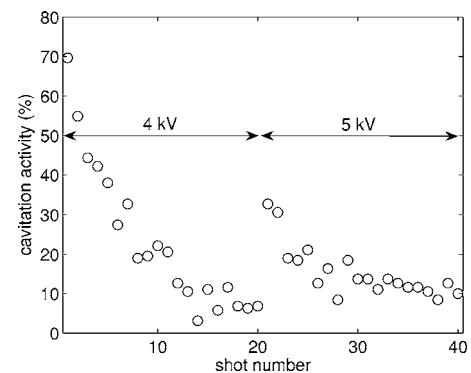


FIG. 7. Cavitation activity for two different tensile stresses, 4 and 5 kV experiments, respectively. Each data point is the mean of three experiments.

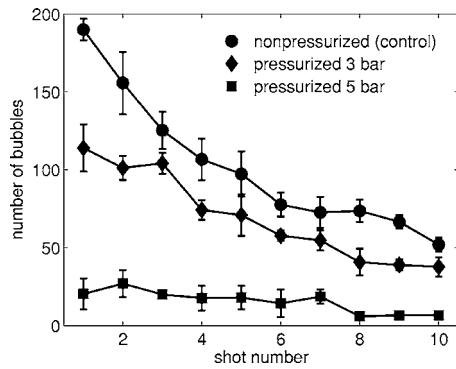


FIG. 8. Temporal evolution of cavitation after preexperimental pressurization. A decrease of cavitation of around 30% has been measured when shooting with 3 kV shots after pressurization with 3 bars (diamonds), compared to the nonpressurized scenario (circles). Pressurization with 5 bars (squares) leads to a cavitation reduction of more than 80%. Every data point is the mean of three experiments (bars depict standard deviation).

the suspension prior to the nucleation experiment. The effect of prepressurization of controlled water-particle-suspensions has not been investigated before, yet it was proposed by Deng *et al.*¹¹ Interestingly, Strasberg found that it is more difficult to obtain cavitation in tap water which had been subjected temporarily to a high pressure.³

The liquid handling during the pressurization step is described in Sec. II B. Two different preexperimental pressurization levels are compared with the case with no pressurization but the same fluid handling steps in Fig. 8. Again, each experiment is repeated three times and the mean number of cavitation bubbles is plotted. The control case, circles in Fig. 8, shows the typical decrease of cavitation activity with shot number. A prepressurization of the suspension with 3 bar absolute pressure for 15 min leads to a significant decrease of cavitation (diamonds in Fig. 8). Cavitation activity is largely diminished with a preexperimental treatment of the suspension with 5 bar overpressure, see squares in Fig. 8. Here, only about 20% of the bubbles are counted as compared to the control.

IV. DISCUSSION

A. Effect of exposure time

Interestingly, the particles (dynoQ735 and dynoQ476, see Fig. 4) which are from the same batch as the ones tested in Marschall *et al.*¹² did not show pronounced cavitation activity in response to the 60 bar peak negative pressure wave (Fig. 2). This is in bold contrast to Keller's vortex-flow nozzle experiment as described in Ref. 12. In that work a negative pressure of 0.87 bar was sufficient to induce cavitation with particles from the same batch. The obvious difference between the two experimental conditions is the exposure duration for the particles to the tensile stress. In the shock wave experiments, particles are exposed only a few microseconds, whereas in the flow cavitation experiments the tensile stress lasts two orders of magnitude longer.²¹ This difference suggests that not only the tensile strength but also the duration of negative pressure exposure is critical for the nucleation process. Our hypothesis is that a longer exposure to tensile stress allows a dynamic rearrangement and possi-

bly a coalescence of gaseous nuclei on the particle surface. These now larger nuclei possess a reduced cavitation threshold and thus explode at smaller absolute pressures.

B. Model

Assuming that each nucleus in the acoustic volume can grow into a cavitation bubble the observed number of bubbles, N_{bub} , should be equal to the number of nuclei present in the observed acoustic volume V_{ob} .

The number of nuclei in the observed acoustic volume is determined from

$$N_{\text{bub}} = \frac{V_{\text{ob}}}{V_{\text{flask}}} N_{\text{nuclei}}, \quad (2)$$

where $V_{\text{flask}} = 75$ ml is the total flask volume and N_{nuclei} the total number of nuclei available in the flask.

The observed acoustic volume is approximated from the experimental geometry with a cylinder, $V_{\text{ob}} = \pi r^2 l$ having a radius $r = 3.6$ mm and a length $l = 14.2$ mm. Initially (exposure number $n = 1$), the number of nuclei in the flask, N_{nuclei} , is related to the number of particles $N_{\text{particles}}$ through the cavitation yield, thus $N_{\text{nuclei}} = N_{\text{particles}} \alpha$, where α is the cavitation yield. We assume that at later stages ($n > 1$) nuclei become used up due to cavitation, thus N_{nuclei} decreases with every shot by a factor of $V_{\text{tav}}/V_{\text{flask}}$. Here, V_{tav} is the total acoustic volume $\pi r^2 l_{\text{flask}}$ where $l_{\text{flask}} = 71$ mm is the length of the acoustic volume in the entire flask. Therefore, the decrease of cavitation nuclei as a function of the exposure number n is given by

$$N_{\text{nuclei}}^{n+1} = \left(1 - \frac{V_{\text{tav}}}{V_{\text{flask}}}\right) N_{\text{nuclei}}^n. \quad (3)$$

Now the number of nucleated bubbles N_{bub} can be calculated from Eq. (2). Here, all model parameters are determined from the experiment and no fitting parameters come into play. The model Eq. (2) gives an exponential decrease in cavitation activity which resembles the trend in the experimental curve reasonably well. It is possible to obtain a very good fit to the measured decay and the model by changing the experimental parameters by no more than by 10%. Yet, we see the good agreement with the measured data only as an indication that indeed a particle is acting as one-time triggerable source of cavitation. This finding underlines the importance of the history of the suspension in cavitation studies, e.g., how many times it has been exposed to a rarefaction wave; and the golden rule of Robert Apfel.²² "Know thy liquid!" applies.

V. CONCLUSION

A novel experimental approach to study cavitation inception within a well controlled environment has been presented. A flask filled with a suspension of clean water and an adjustable number of particles is exposed to a single shock wave-rarefaction wave cycle. At a peak negative pressure amplitude of 60 bar, hydrophobic and corrugated polymer particles facilitate cavitation inception, while smooth and hydrophilic particles do not enhance cavitation activity. In the case of polyamide, around 80% of the particles nucleate after

the passage of the first shock wave. For successive shock waves, the number of cavitation bubbles decreases exponentially, which is shown by running a simple cavitation nucleation model. This exponential decrease suggests that particles have a limited number of nucleation sites which are consumed during the experiment. Therefore the level of cavitation activity reflects the history of the liquid. It was also found that more bubbles are observed with increasing negative pressure. This suggests that the nucleation sites on the particles have varying cavitation thresholds. Finally, it was observed that the cavitation yield decreases when the suspension is prepressurized suggesting that the cavitation nucleus is of gaseous origin.

ACKNOWLEDGMENTS

We are grateful to Professor Knud Aage Mørch and Professor Detlef Lohse for fruitful discussions and Gert-Wim Bruggert for technical support. The work is partly financed by “Stichting Technische Wetenschappen (STW),” “Stichting voor Fundamenteel Onderzoek der Materie (FOM),” and the “Nederlandse Organisatie voor Wetenschappelijk Onderzoek (NWO).”

¹E. N. Harvey, D. K. Barnes, W. D. McElroy, A. H. Whiteley, D. C. Pease, and K. W. Cooper, “Bubble formation in animals,” *J. Cell. Comp. Physiol.* **24**, 1–22 (1944).

²M. Greenspan and C. E. Tschiegg, “Radiation-induced acoustic cavitation: Apparatus and some results,” *J. Res. Natl. Bur. Stand., Sect. C* **71**, 299–312 (1967).

³M. Strasberg, “Onset of ultrasonic cavitation in tap water,” *J. Acoust. Soc. Am.* **31**, 163–176 (1959).

⁴R. E. Apfel, “The role of impurities in cavitation-threshold determination,” *J. Acoust. Soc. Am.* **48**, 1179–1186 (1970).

⁵L. A. Crum, “Tensile strength of water,” *Nature (London)* **278**, 148–149 (1979).

⁶K. A. Mørch, “Cavitation nuclei and bubble formation—A dynamic

liquid-solid interface problem,” *J. Fluoresc.* **122**, 494–498 (2000).

⁷A. A. Atchley and A. Prosperetti, “The crevice model of bubble nucleation,” *J. Acoust. Soc. Am.* **86**, 1065–1084 (1989).

⁸W. J. Galloway, “An experimental study of acoustically induced cavitation in liquids,” *J. Acoust. Soc. Am.* **26**, 849–857 (1954).

⁹R. A. Roy, S. I. Madanshetty, and R. E. Apfel, “An acoustic backscattering technique for the detection of transient cavitation produced by microsecond pulses of ultrasound,” *J. Acoust. Soc. Am.* **87**, 2451–2458 (1989).

¹⁰S. I. Madanshetty, “A conceptual model for acoustic microcavitation,” *J. Acoust. Soc. Am.* **98**, 2681–2689 (1995).

¹¹C. X. Deng, Q. Xu, R. E. Apfel, and C. K. Holland, “Inertial cavitation produced by pulsed ultrasound in controlled host media,” *J. Acoust. Soc. Am.* **100**, 1199–1208 (1996).

¹²H. B. Marschall, K. A. Mørch, A. P. Keller, and M. Kjeldsen, “Cavitation inception by almost spherical solid particles in water,” *Phys. Fluids* **15**, 545–553 (2003).

¹³S. I. Madanshetty and R. E. Apfel, “Acoustic microcavitation: Enhancement and applications,” *J. Acoust. Soc. Am.* **90**, 1508–1514 (1991).

¹⁴S. I. Madanshetty, R. Roy, and R. E. Apfel, “Acoustic microcavitation—Its active and passive acoustic detection,” *J. Acoust. Soc. Am.* **90**, 1515–1526 (1991).

¹⁵A. A. Atchley, L. A. Frizzell, R. E. Apfel, C. K. Holland, S. Madanshetty, and R. A. Roy, “Thresholds for cavitation produced in water by pulsed ultrasound,” *Ultrasonics* **26**, 280–285 (1988).

¹⁶M. Arora, C. D. Ohl, and K. A. Mørch, “Cavitation inception on micro-particles: A self-propelled particle accelerator,” *Phys. Rev. Lett.* **92**, 174501–1–4 (2004).

¹⁷M. Arora, L. Junge, and C. D. Ohl, “Cavitation cluster dynamics in shock-wave lithotripsy. 1. Free field,” *Ultrasound Med. Biol.* **31**, 827–839 (2005).

¹⁸Y. A. Pishchalnikov, O. A. Sapozhnikov, and M. R. Bailey, “Cavitation selectively reduces the negative-pressure phase of lithotripter shock pulses,” *ARLO* **6**, 280–286 (2005).

¹⁹O. A. Sapozhnikov, V. A. Khokhlova, M. R. Bailey, J. C. Williams, J. A. McAteer, R. O. Cleveland, and L. A. Crum, “Effect of overpressure and pulse repetition frequency on cavitation in shock wave lithotripsy,” *J. Acoust. Soc. Am.* **112**, 1183–1195 (2002).

²⁰P. S. Epstein and M. S. Plesset, “On the stability of gas bubbles in liquid-gas solutions,” *J. Chem. Phys.* **18**, 1505–1509 (1950).

²¹K. A. Mørch, private communication.

²²R. E. Apfel, “Acoustic cavitation inception,” *Ultrasonics* **22**, 168–173 (1984).